Cryopreserved Human Precision-Cut Lung Slices as a Bioassay for Live Tissue Banking

A Viability Study of Bronchodilation with Bitter-Taste Receptor Agonists

Yan Bai[1], Nandini Krishnamoorthy[2], Kruti R. Patel[1], Ivan Rosas[2], Michael J. Sanderson[3], and Xingbin Ai[1,2]

[1]Pulmonary, Allergy, Sleep and Critical Care Medicine, Boston University School of Medicine, Boston, Massachusetts; [2]Pulmonary and Critical Care Medicine, Brigham and Women's Hospital, Boston, Massachusetts; and [3]Department of Microbiology and Physiological Systems, University of Massachusetts Medical School, Worcester, Massachusetts

Abstract

Human precision-cut lung slices (hPCLSs) provide a unique *ex vivo* model for translational research. However, the limited and unpredictable availability of human lung tissue greatly impedes their use. Here, we demonstrate that cryopreservation of hPCLSs facilitates banking of live human lung tissue for routine use. Our results show that cryopreservation had little effect on overall cell viability and vital functions of immune cells, including phagocytes and T lymphocytes. In addition, airway contraction and relaxation in response to specific agonists and antagonists, respectively, were unchanged after cryopreservation. At the subcellular level, cryopreserved hPCLSs maintained Ca^{2+}-dependent regulatory mechanisms for the control of airway smooth muscle cell contractility. To exemplify the use of cryopreserved hPCLSs in smooth muscle research, we provide evidence that bitter-taste receptor (TAS2R) agonists relax airways by blocking Ca^{2+} oscillations in airway smooth muscle cells. In conclusion, the banking of cryopreserved hPCLSs provides a robust bioassay for translational research of lung physiology and disease.

Keywords: human precision-cut lung slices; cryopreservation; Ca^{2+} oscillations; bitter-taste receptor; biobank

The use of human precision-cut lung slices (hPCLSs) is becoming widely accepted as a research tool to investigate the physiological and pharmacological responses of normal and diseased lung tissue (1, 2). PCLSs retain the organizational features of the *in vivo* lung, while providing microscopic access for individual cells (3–6). Despite these advantages, the use of hPCLSs is confounded by the unpredictable and limited availability of human tissue. Ironically, when a human lung is available, the amount is often too much for use within the period of tissue viability. Establishment of methods that allow long-term storage of live hPCLSs will empower experimentation using human tissue.

Cryopreservation has been reported to store live biological samples with varying success (7, 8), and its application to mouse PCLSs (mPCLSs) was previously assessed (9). This study employed histology and phase–contrast imaging to show that the lung tissue integrity and agonist-induced airway contraction were retained in cryopreserved mPCLSs. This suggests that a similar, slow-freezing, and fast-thawing protocol may preserve hPCLSs for "live" lung tissue banking. However, because freezing can induce cryoinjury, and cryoprotective agents may have side effects (10–12), it is essential to evaluate viability and key cell functions at both cellular and subcellular levels in cryopreserved hPCLSs before adopting this approach.

In this study, we extensively characterized the viability and vital functions of phagocytes, lymphocytes, and airway smooth muscle cells (ASMCs) in cryopreserved hPCLSs. We also investigated the action of bitter-taste receptor (TAS2R) agonists, potentially novel bronchodilators

(Received in original form September 15, 2015; accepted in final form October 8, 2015)

This work was supported by a T32 training grant National Institutes of Health grant T32 HL007035 (Y.B.), an American Asthma Foundation grant (X.A.), and National Institutes of Health grant HL103405 (M.J.S.).

Author Contributions: Y.B. performed preparation, cryopreservation, and culture of human precision-cut lung slices, experiments of phagocytosis and airway contraction, Ca^{2+} signaling and Ca^{2+} sensitivity of airway smooth muscle cells; N.K. and K.R.P. performed the flow cytometry assay of lymphocyte activation and proliferation; I.R. contributed to the collection of human lung samples and experimental design; M.J.S. and X.A. conceived the overall experimental design and research plan; all authors contributed to experimental design, data interpretation, and manuscript preparation.

Correspondence and requests for reprints should be addressed to Michael J. Sanderson, Ph.D., Department of Microbiology and Physiological Systems, University of Massachusetts Medical School, Worcester, MA 01655. E-mail: michael.sanderson@umassmed.edu

This article has an online supplement, which is accessible from this issue's table of contents at www.atsjournals.org

Am J Respir Cell Mol Biol Vol 54, Iss 5, pp 656–663, May 2016

Originally Published in Press as DOI: 10.1165/rcmb.2015-0290MA on November 9, 2015
Internet address: www.atsjournals.org

Clinical Relevance

Our study demonstrates a promising solution to overcome the scarce availability of human lung tissue for translational research by banking human precision-cut lung slices (hPCLSs) with cryopreservation. The study verified well-maintained cell viability, tissue architecture, and intact activities of epithelia, phagocytes, lymphocytes, and airway smooth muscle cells in frozen–thawed hPCLSs. This is, to our knowledge, the first comprehensive evaluation of the effect of cryopreservation on a human heterogeneous tissue section with a large variety of cell types. To emphasize the bioassay utility of cryopreserved hPCLSs, we characterize the mechanism of action of bitter-taste receptor agonists, a novel class of bronchodilators, as an inhibition of Ca^{2+} oscillations in airway smooth muscle. Thus, the application of cryopreserved hPCLSs will profoundly empower the *ex vivo* immunological, physiological, and pharmacological studies on a variety of lung diseases from the molecular to the integrated tissue level.

(13, 14), using cryopreserved hPCLSs. Our findings indicate that cryopreserved hPCLSs provide an invaluable tool for studies of lung physiology and disease mechanisms and for drug screening.

Materials and Methods

Reagents

Ultrapure agarose of low melting point was obtained from GIBCO–Invitrogen (Waltham, MA). Hanks' balanced salt solution (HBSS) with calcium and magnesium was obtained from Corning (Tewksbury, MA). All chemicals were obtained from Sigma-Aldrich (St. Louis, MO). Oregon green 488 BAPTA-1-AM was purchased from Molecular Probes–Invitrogen Corp. (Eugene, OR). Dulbecco's modified Eagle medium (DMEM)/F12, RPMI 1640, antibiotics, antimycotics, and pHrodo Red *Eschericia coli* BioParticles Conjugate were purchased from Life Technologies (Carlsbad, CA). Alexa Fluor 488–conjugated anti-human CD11c antibody, carboxyfluorescein succinimidyl ester (CFSE) Cell Division Tracker Kit, IL-2, and anti-human CD3, CD28, allophycocyanin (APC) anti-human CD4, phycoerythrin (PE) anti-human CD8, APC/cyanine 7 (Cy7) anti-human CD69, PE/Cy7 anti-human CD25 were purchased from Biolegend (San Diego, CA).

hPCLS Preparation

Healthy donor lungs that were declined for transplantation at Brigham and Women's Hospital (Boston, MA) were used. The right middle and lower lobes were inflated by injecting 2% warm (37°C) low-melting agarose–HBSS solution (~1 L) via a catheter cannulated in the right intermediate bronchus. After complete solidification of agarose in the inflated lobes on ice, tissue blocks of approximately 1 cm in each dimension were prepared. Lung slices (250 μm thick) were cut perpendicularly to the visible airway with a vibratome (VF-300; Precisionary Instruments, Greenville, NC) at room temperature in HBSS. After overnight incubation at 37°C in 5% CO_2 and DMEM/F-12 supplemented with antibiotics, the collected lung slices were placed in cryovials with DMEM/F-12 containing 10% DMSO (three slices/ml/vial), stored in 100% isopropyl alcohol–filled Nalgene Mr. Frosty Freezing Container (Thermo Fisher Scientific, Cambridge, MA) and subsequently frozen at −80°C. After overnight freezing, cryovials were transferred to liquid nitrogen for long-term storage. On the day of the experiment, each cryovial was thawed rapidly in a 37°C water bath. hPCLSs were then removed to fresh DMEM/F-12, washed twice with medium, and cultured for 6 hours before experiments. A total of three healthy donor lungs were used in our study.

Measurement of Airway Contraction by Phase–Contrast Digital Microscopy

hPCLSs were placed in a 12-well culture plate, covered with a nylon mesh with a central hole to expose the airway, and secured in place by a stainless steel washer. Reaction solution (2 ml) was sequentially added and removed by gentle suction. Images were taken at time zero, 10 minutes after exposure to a contractile agent, and 15 minutes after exposure to an airway relaxant with an inverted microscope (Nikon Eclipse TS 100; Nikon, Tokyo, Japan), a 4× objective, and a Nikon DS-Ri2 camera. Alternatively, contraction and relaxation of airways in hPLCSs were measured as previously described (5, 15). Image analysis was performed with Image J software (National Institutes of Health, Bethesda, MD).

Intracellular Ca^{2+} Imaging in Airway Smooth Muscle of hPCLSs by Two-Photon Fluorescence Microscopy

hPCLSs were loaded with Ca^{2+} indicator, Oregon green BAPTA-1-AM, as previously described (5, 15). Fluorescence images were recorded at 30 images per second with a custom-built two-photon laser scanning microscope and analyzed by Video Savant software (IO Industries, London, ON, Canada) with custom-written scripts. Line-scan images were compiled using Image J software.

Phagocytosis Analysis

Thawed slices were incubated with pHrodo red–conjugated *E. coli* bioparticle suspension (0.5 mg/ml in HBSS, one slice per 500 μl solution) at 37°C and 5% CO_2 for 90 minutes and examined with a Nikon Eclipse TS 100 epifluorescence microscope at the excitation wavelength of 530–580 nm. $CD11c^+$ cells in thawed hPCLSs were identified after 2-hour incubation of slices with Alexa Fluor 488–conjugated anti-CD11c antibody (4 μg/ml) at room temperature and examined at the excitation wavelength of 470–510 nm with the same epifluorescence microscopy.

Lymphocyte Activation and Proliferation

Thawed hPCLSs were cultured in a 24-well culture plate with RPMI media supplemented with 10% FBS, antibiotics, and antimycotics (one slice/ml in each well). The medium was changed every 48 hours. To stimulate lymphocytes, the wells were precoated with anti-CD3 (2 μg/ml) and anti-CD28 (8 μg/ml) antibodies. IL-2 (10 ng/ml) was added to the culture medium on Day 3. After a total of 6 days in culture, cells on the bottom of the culture plate were collected after collagenase (100 μg/ml) treatment for 5 minutes. Cells were then subjected to flow cytometry analysis for the expression of lymphocyte activation markers. To evaluate lymphocyte proliferation, cells were labeled with CFSE followed by stimulation with IL-2, anti-CD3, and anti-CD28 precoated on the culture plate for 48 hours before flow cytometry evaluation.

Flow Cytometry

The cells were incubated with antibodies against CD4, CD8, CD25 and CD69 on ice

for 30 minutes before flow cytometry analysis. All antibodies were used at 1:100 dilution. All flow cytometry experiments were performed using a BD FACS Canto II flow cytometer (Becton Dickinson, Franklin Lakes, NJ). A total of 100,000 events were recorded for each antibody. Data were analyzed using FlowJo software (Tree Star, Ashland, OR).

Statistical Analysis

Data are expressed as the mean value (±SEM). Significance was determined at P values less than 0.05 by Student's t test. Statistical analyses were performed using GraphPad Prism 5 for Windows (GraphPad Software, Inc., La Jolla, CA).

Results

Cryopreservation Does Not Affect Cell Viability

To access cell viability, we cultured thawed hPCLSs (one slice/ml) over time and tested the media, which was exchanged every 48 hours, for lactate dehydrogenase (LDH). The control treatment of hPCLSs with 0.1% triton to rupture cell membranes resulted in a large increase in LDH. After hPCLS thawing, LDH levels were low after 24 hours and remained low for 10 days of prolonged culture (*see* Figure E1 in the online supplement). These results infer that there is minimal cell death or the induction of cell apoptosis in the post-thaw period. In addition, microscopy showed that the airway and surrounding parenchyma were structurally intact (Figure 2A and Movie E1 in the online supplement) and that there was ciliary beating on the airway epithelium (data not shown).

Function of Phagocytes and Lymphocytes in Cryopreserved hPCLSs

Although low cell death is an excellent indication of viable cryopreserved hPCLSs, the assessment of specific responses of individual cells is a better criterion for the preservation of cell function. Because resident immune cells play a critical role in host defense (16–20), we chose to evaluate the vital functions of immune cells in cryopreserved hPCLSs. We first assessed phagocytosis, a critical process for clearance of infection. For this assay, we incubated cryopreserved hPCLSs with *E. coli* particles conjugated with pHrodo red. Once engulfed into the acidic phagosome, *E. coli* particles yielded dramatically intensified fluorescence, thereby permitting direct visualization of phagocytosis by resident phagocytes. After incubation at 37°C for 90 minutes, multiple phagocytes with bright intracellular fluorescent particles were observed in cryopreserved hPCLSs (Figure 1A, *left panel*), indicating active phagocytosis. We further examined

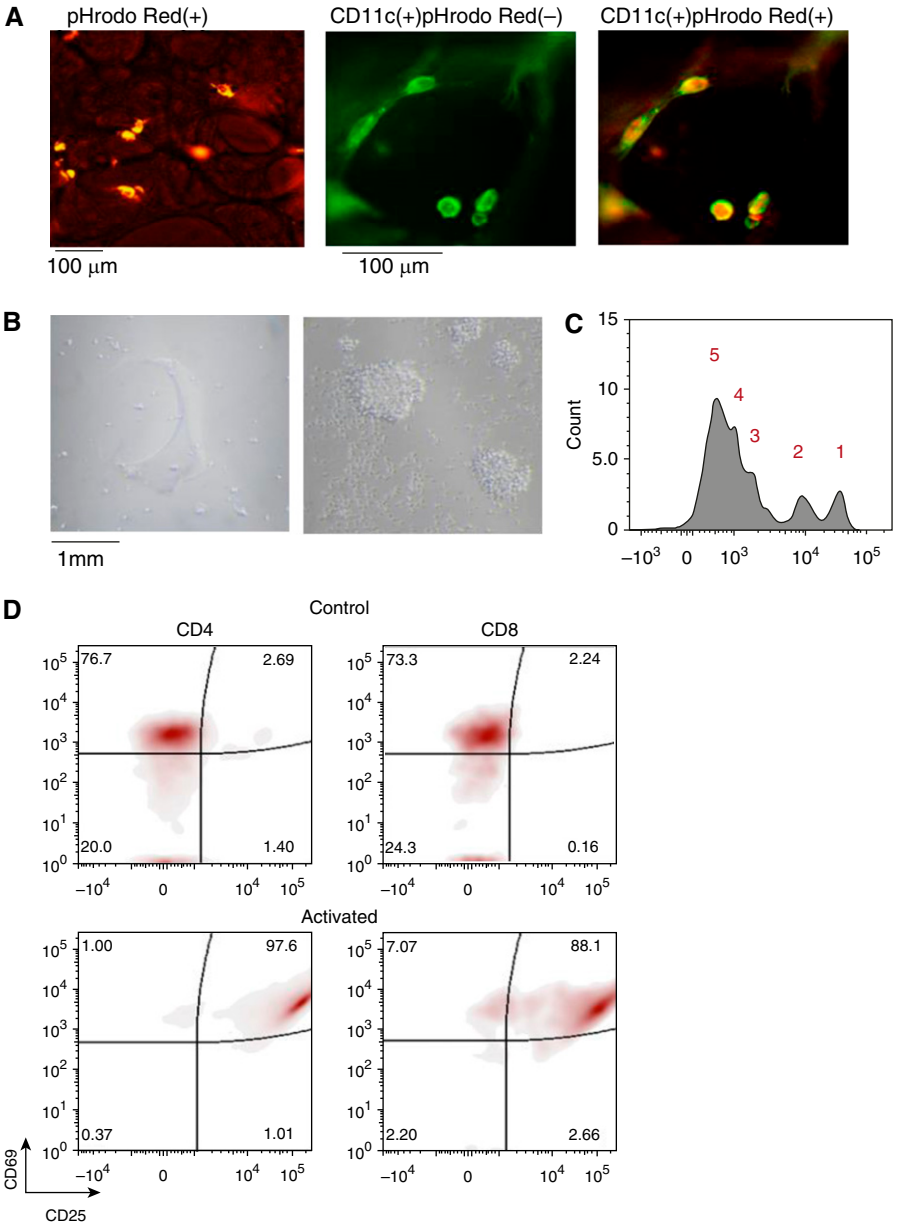

Figure 1. Immune cell function in cryopreserved human precision-cut lung slices (hPCLSs). (*A*) Phagocytosis assay in thawed hPCLSs. *Left panel* shows a representative image of intracellular fluorescence of *in situ* phagocytes after 90-minute incubation of hPCLSs with pHrodo red–conjugated *Escherichia coli* particles indicative of active phagocytosis. Representative fluorescence images show the same hPLCS stained with CD11c antibody (*middle panel*, in *green*), followed by phagocytosis assay (*right panel*). A large majority of $CD11c^+$ cells had intracellular pHrodo red *E. coli* particles. (*B*) Representative images showing (*left panel*) cells on the culture plate after thawed hPCLSs were cultured for 6 days in control media (RPMI + 10% FBS) or (*right panel*) under dual activation by IL-2 (10 ng/ml) and anti-CD3 (2 μg/ml) plus anti-CD28 (8 μg/ml) antibodies coated on the bottom of culture plates to stimulate lymphocytes. (*C*) Proliferation analysis of CD4 gated lymphocytes with carboxyfluorescein succinimidyl ester dilution and flow cytometry. The number of cell division was marked. (*D*) Flow cytometry analysis of lymphocytes on the plates of control and activated hPCLS cultures. Cells gated with CD4 and CD8 were assayed for their activation status by their expression of CD69 and CD25.

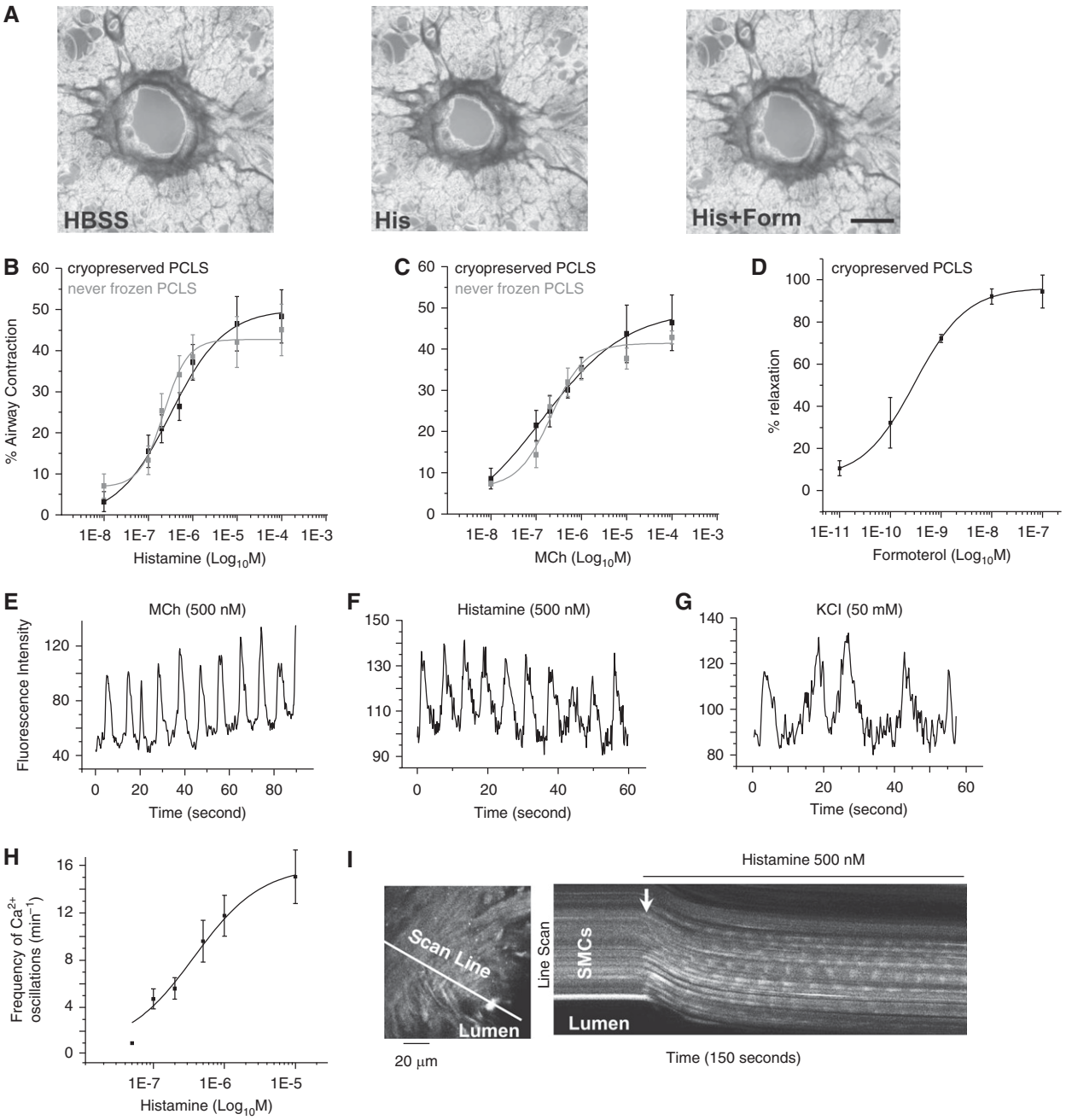

Figure 2. Contraction, relaxation, and intracellular Ca^{2+} concentration ($[Ca^{2+}]_i$) in airway smooth muscle cells (ASMCs) of cryopreserved hPCLSs. (*A*) Phase–contrast images of a human airway in a cryopreserved hPCLS in Hanks' balanced salt solution (HBSS; *left*), after exposure to histamine (His; 500 nM) (*middle*), or histamine with formoterol (His + Form; 10 nM) (*right*). *Scale bar*, 1 mm. (*B*) The mean concentration–airway contraction (%) response to histamine in cryopreserved hPCLSs (*black line*, $EC_{50} = 314.9 \pm 81.2$ nM) and never-frozen hPCLSs (*gray line*, $EC_{50} = 221.8 \pm 62.5$ nM). (*C*) Similar response curve to methacholine (MCh) in cryopreserved hPCLSs (*black line*, half maximal effective concentration [EC_{50}] = 166 ± 47nM) and never-frozen hPCLSs (*gray lines*, $EC_{50} = 191 \pm 54$ nM) ($n = 8$ cryopreserved airways and 5–7 never-frozen airways from two human samples). Airway area reduction was measured 10 minutes after agonist administration. Each *point* represents mean (±SEM). Data were fitted with a sigmoidal curve. (*D*) The mean concentration–relaxation (% normalized to initial contraction) response to formoterol in cryopreserved hPCLS ($n = 8$ airways from two human samples, measured 15 min after administration). Each *point* represents the mean (±SEM). Data were fitted with a sigmoidal curve. (*E–G*) Representative intracellular Ca^{2+} signaling of individual ASMCs in response to MCh (500 nM), histamine (500 nM), and KCl (50 mM). The oscillatory elevation of fluorescence intensity indicates the cyclic increase of $[Ca^{2+}]_i$. (*H*) The Ca^{2+} oscillation frequency at different concentrations of histamine. Higher concentrations of histamine induced faster Ca^{2+} oscillations. Data are means (±SEM), fitted with a sigmoidal curve ($n = 10$ airways from three human samples at each concentration). (*I*) *Left panel*: a representative image of ASMCs loaded with Oregon green 488 BAPTA-1 in a segment of the airway wall. *Right panel*: a line-scan analysis showing changes in fluorescence intensity of several adjacent ASMCs along a scan line across the airway wall to 500 nM histamine over time. The simultaneous contraction of ASMC bundle toward airway lumen is indicated by the *white arrow*.

phagocytes for CD11c expression by immunostaining (Figure 1A, *middle panel*). CD11c labels alveolar macrophages and dendritic cells, two types of phagocytes (21). Indeed, a majority of cells that exhibited phagocytic activities in cryopreserved hPCLSs were $CD11c^{+}$ (Figure 1A, *right panel*). To our knowledge, this is the first demonstration of phagocyte activities *in situ* in hPCLSs.

We then tested activation and proliferation of lymphocytes in cryopreserved hPCLSs. During 6 days in culture, a few cells migrated out from hPCLSs to the plate (Figure 1B, *left panel*). However, when slices were stimulated with IL-2 and the antibodies against CD3 and CD28 precoated on the plate to mimic antigen-presenting cells, a large number of cell clones appeared on the plates (Figure 1B, *right panel*). We assessed these cells for activated lymphocyte cell surface markers CD69 and CD25 by flow cytometry. In unstimulated cultures, cells positive for CD69 and CD25 accounted for 2.69% CD4 T cells and 2.24% CD8 T cells. These percentages increased to 97.6% CD4 T cells and 88.1% CD8 T cells after stimulation (Figure 1D). Lymphocyte proliferation in stimulated cultures was validated by CFSE staining (Figure 1C). These findings demonstrate that viable, responsive lymphocytes are maintained in hPCLSs after cryopreservation. Together, cryopreserved hPCLSs may serve as a reliable *ex vivo* model to study innate immunity in lung physiology and disease.

Contractile and Relaxant Responses of Airways in Cryopreserved hPCLSs

PCLSs have been widely used for studies of airway contractility and mechanisms of airway hyperreactivity in asthma (4, 5, 9, 15, 22, 23). Because airway contraction requires the coordinated activity of ASMCs, this multicellular response requires high rates of ASMC viability after cryopreservation. To confirm that cryopreserved airways in hPCLSs were able to match this exacting criterion, airway responses to contractile agonists were investigated (Movie E1; Figure 2). In response to histamine (His; 10^{-8} M to 10^{-4} M) or methacholine (MCh; 10^{-8} M to 10^{-4} M), airways contracted in proportion to the agonist concentration in a manner that was virtually indistinguishable from never-frozen hPCLSs (Figures 2B and 2C). For hPCLSs to serve as a valid model for asthma research, the airways

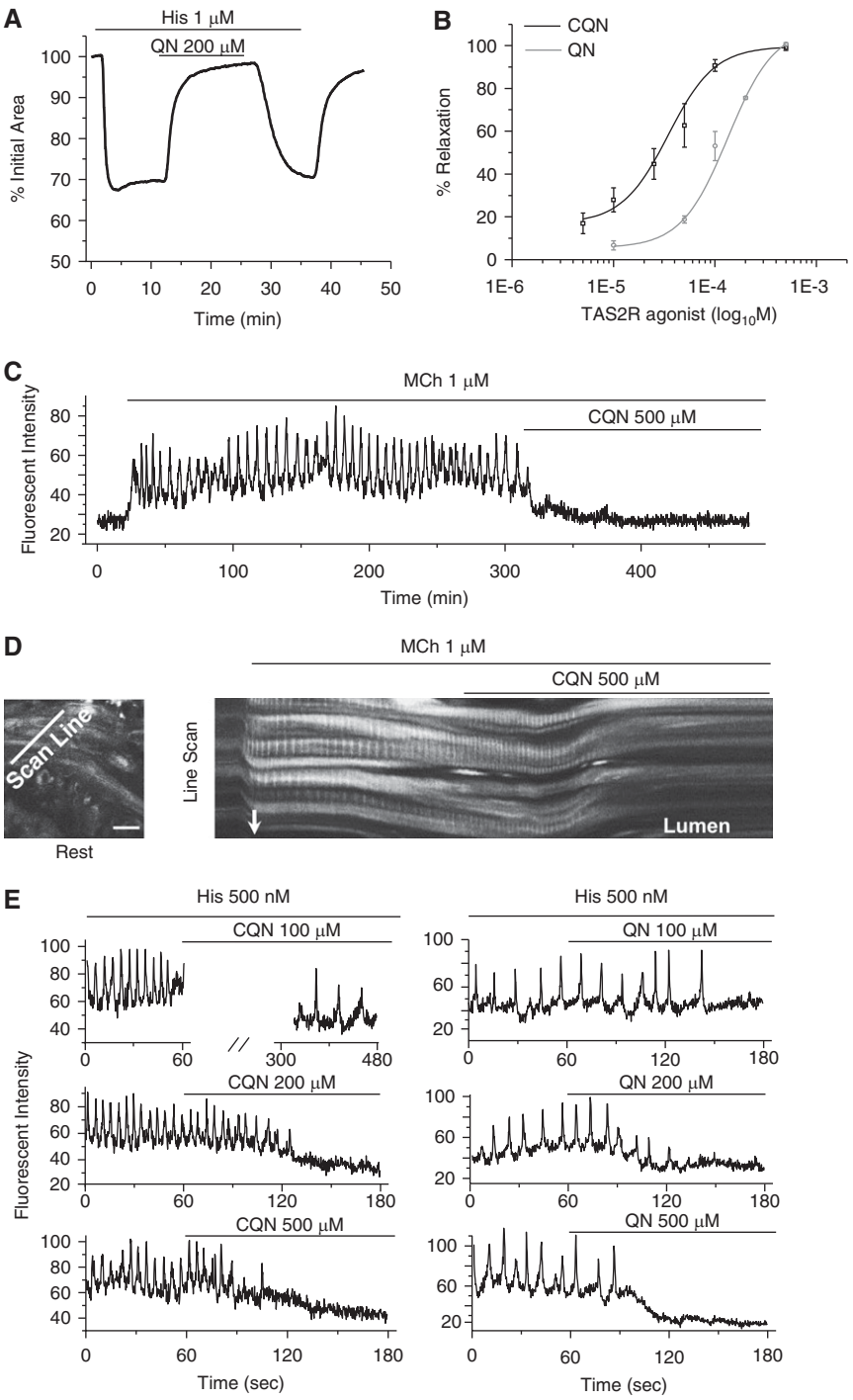

Figure 3. Effect of bitter-taste receptor agonists on airway contraction and ASMC Ca^{2+} signaling. (*A*) Representative airway response showing the relaxant effect of 200 μM quinine (QN) on an airway contracted with 1 μM histamine. (*B*) The mean relaxant responses (% normalized to the initial airway contraction) of airways contracted with 1 μM histamine to increasing concentrations of chloroquine (CQN; *black line*, $EC_{50} = 40.2 \pm 7.4$ μM) and QN (*gray line*, $EC_{50} = 114.7 \pm 24.2$ μM). Data are means (±SEM) fitted with a sigmoidal curve ($n = 5$ airways from two human samples at each concentrations). (*C*) A representative trace showing the inhibition of MCh-induced Ca^{2+} oscillations by CQN in an ASMC. (*D*) *Left panel*: a representative image of ASMCs loaded with Ca^{2+} dye within a segment of airway wall at rest. *Right panel*: changes in fluorescence intensity of multiple ASMCs along the indicated scan line across the airway wall (*left panel*) over time. MCh induced an asynchronous oscillatory elevation of fluorescence intensity in adjacent ASMCs with the airway wall moving toward

should also demonstrate the well known responses of *in vivo* airways to β_2-adrenergic receptor agonists that are commonly used for asthma therapy. Consequently, we investigated the airway response to formoterol, a long-acting β_2-adrenergic receptor agonist. Airways in hPCLSs were first contracted with 500 nM His, the subsequent exposure to formoterol induced dose-dependent airway relaxation (half maximal effective concentration [EC_{50}] = 0.6 nM; Figure 2D). This response was similar to that observed in airways of never-frozen hPCLSs, as previously published (24). These observations provide strong evidence that ASMCs in cryopreserved hPCLSs are highly viable and functional. These results also indicate that the mechanical properties of hPCLSs with respect to tethering that limit contraction and mediate airway relaxation remain unchanged.

Ca^{2+} Signaling of ASMCs in Cryopreserved hPCLSs

Intracellular Ca^{2+} oscillations are key signals in the control of agonist-induced contraction (5, 15, 23, 25, 26). To determine if this regulatory mechanism was unchanged by cryopreservation, two-photon microscopy was used to monitor the fluorescence of a Ca^{2+} indicator, Oregon green BAPTA-1, to report the intracellular Ca^{2+} concentration ($[Ca^{2+}]_i$) of ASMCs. Similar to our previous findings in never-frozen hPCLSs, we found in cryopreserved hPCLSs that His, MCh, and high K^+ induced oscillatory increases of $[Ca^{2+}]_i$ (Figures 2E–2G); the frequency of the Ca^{2+} oscillations increased from 1 to approximately 15 per minute when the His concentration was increased from 50 nm to 10 μM (Figure 2H). In an individual ASMC, Ca^{2+} oscillations appeared as waves that propagated along the cell length (Movie E2). These Ca^{2+} oscillations in ASMCs were accompanied by constriction of the airway (Figure 2I). These observations validate that cryopreserved hPCLSs have normal Ca^{2+}-dependent regulation of ASMC contraction. In addition, Ca^{2+} sensitivity of ASMCs in cryopreserved hPCLSs was also unchanged (Figure E2).

TAS2R Agonists Relax Human Airways by Inhibiting Ca^{2+} Oscillations of ASMCs

With this confirmation that cryopreserved hPCLSs are a reliable substitute for never-frozen hPCLSs to evaluate ASMC function, we investigated the effects of TAS2R agonists, chloroquine (CQN) and quinine (QN), on contracted human airways and their associated Ca^{2+} signaling in ASMCs. hPCLSs were contracted with 1 μM His and the subsequent exposure to QN (or CQN) induced a rapid airway relaxation (Figure 3A). The removal of QN (or CQN) resulted in the recontraction of the airway. The bronchodilation was concentration dependent for CQN (EC_{50} = 40 μM) and QN (EC_{50} = 114 μM), and both agonists led to near full relaxation at 500 μM (Figure 3B). When the unstimulated hPCLSs were exposed to 1 mM CQN, no focal or global increases of Ca^{2+} were observed during 5 minutes of CQN exposure. After CQN removal, the same airway displayed asynchronous Ca^{2+} oscillations in ASMCs in response to 1 μM MCh. The subsequent exposure to 500 μM CQN completely stopped these Ca^{2+} oscillations within 1 minute (Movie E3, Figure 3C), and this was associated with relaxation of ASMCs and dilation of the airway lumen (Figure 3D). When the Ca^{2+} oscillations ceased in the presence of CQN, no focal events of Ca^{2+} sparks were observed to maintain the low $[Ca^{2+}]_i$. Both CQN and QN exhibited similar concentration-dependent inhibition on Ca^{2+} oscillations stimulated with 500 nM His (Figure 3E). Their suppressive effects were reversible, as the Ca^{2+} oscillations resumed after CQN or QN removal. Taken together, these findings suggested that TAS2R agonists relaxed contracted ASMCs via the inhibition of the Ca^{2+} oscillations.

Discussion

Cryopreservation of tissue would appear to face many problems, such as distortion of tissue architecture, uneven freezing, or various cryoprotectant requirements by different cell types within the tissue (27–30). Thus, it would appear that tissue cryopreservation would be extremely challenging to optimize with a single freezing condition for all cell types. Nevertheless, in the present study, we report that cryopreservation of hPCLSs is highly successful, as judged by our evaluation of the extent of cell death, ciliary activity, and the viability of heterogeneous immune cell populations and airway SMC reactivity. Although the reasons for this success were not determined, it would seem likely that the large surface area–to–tissue mass ratio of the thin lung section, as well as the uniform distribution of agarose throughout the alveoli, facilitate rapid and uniform freezing and thawing.

Our study provides the first characterization of immune cells in cryopreserved hPCLSs. In addition to robust phagocytosis, significant increases in CD25 and CD69 expression and cell cycling after lymphocyte stimulation verified that phagocytes and lymphocytes from cryopreserved hPCLSs were healthy and responsive. Whether other immune cell types are viable in cryopreserved hPCLSs warrants future studies. Compared with cell cultures, lung slices provide intact tissue structure and cell–cell interaction that are critical for immune cell behavior. In this context, cryopreserved hPCLSs may serve as an informative model to investigate the onset, maintenance, and modulation of innate immune responses in normal and diseased lungs.

A major application of PCLSs was the investigation of the contractile regulation of intrapulmonary small airways to obtain a better understanding of ASMC physiology and to develop new therapeutic approaches for airway diseases, such as asthma. Previous studies clearly demonstrated two major regulatory mechanisms of ASMC contractility (i.e., mechanisms dependent on Ca^{2+} signaling and Ca^{2+} sensitivity in both never-frozen mPCLSs and hPCLSs). It has also been established that

Figure 3. (Continued). the lumen (*white arrow*). CQN stopped the Ca^{2+} oscillation, reduced the intracellular Ca^{2+} fluorescence intensity, and reversed the displacement of airway wall. *Scale bar*: 25 μm. (*E*) Representative Ca^{2+} responses of ASMCs to increasing concentrations of CQN (*left panels*) and QN (*right panels*) on 500 nM histamine-induced Ca^{2+} oscillations. A concentration of 100 μM CQN reduced the frequency of the Ca^{2+} oscillations, from 11 min^{-1} to 1–2 min^{-1} after 5 minutes. Higher concentrations of CQN completely stopped the Ca^{2+} oscillation. Higher concentrations of CQN took less time to abolish the Ca^{2+} signaling. A similar concentration-dependent inhibition of histamine-induced Ca^{2+} oscillation was observed with QN (two human lungs with n = 2–3 airways from each lung).

agonist-induced ASMC contraction is mediated by Ca^{2+} oscillations and an increase in Ca^{2+} sensitivity (24, 31–38). By contrast, the adrenergic receptor agonist, formoterol, relaxed contracted human airways by initially decreasing ASMC Ca^{2+} sensitivity followed by the inhibition of Ca^{2+} oscillations with increasing formoterol concentrations (24, 39–43). In this study, a similar regulation of human ASMCs was confirmed using cryopreserved hPCLSs. In addition, we have now characterized how TAS2R receptor agonists modify the Ca^{2+}-dependent regulation of ASMCs to induce bronchodilation. In isolated primary human ASMCs, it was reported that TAS2R agonists induced elemental Ca^{2+} events (sparks), which were thought to induce membrane hyperpolarization via activation of large conductance Ca^{2+}-dependent K^+ channel to inhibit Ca^{2+} influx and thereby relax ASMCs (44, 45). In contrast, experiments with mPCLSs suggested that TAS2R agonists slowed or completely stopped Ca^{2+} oscillations by inhibiting the inositol trisphosphate (IP_3) receptors (46). Our experiments with cryopreserved hPCLSs show, for the first time, that TAS2R agonists also inhibit Ca^{2+} oscillations in human ASMCs to induce airway relaxation. These findings indicate that the fundamental role of TAS2R agonists on Ca^{2+} mobilization is via suppression of the phospholipase C-inositol trisphosphate (PLC-IP_3) pathways in ASMCs.

In summary, the present study confirms that cryopreservation of hPCLSs has little adverse effects on tissue architecture or viability of various residential cells. It establishes a firm foundation for banking hPCLSs, which will greatly enhance the exploitation of hPCLSs for translational research. ■

Author disclosures are available with the text of this article at www.atsjournals.org.

Acknowledgments: The authors thank Dr. Junqing Cui for help with the initial immune cell assays.

References

1. Sanderson MJ. Exploring lung physiology in health and disease with lung slices. *Pulm Pharmacol Ther* 2011;24:452–465.
2. Morin JP, Baste JM, Gay A, Crochemore C, Corbière C, Monteil C. Precision cut lung slices as an efficient tool for *in vitro* lung physio-pharmacotoxicology studies. *Xenobiotica* 2013;43:63–72.
3. Jain N, Miu B, Jiang JK, McKinstry KK, Prince A, Swain SL, Greiner DL, Thomas CJ, Sanderson MJ, Berg LJ, *et al*. CD28 and ITK signals regulate autoreactive T cell trafficking. *Nat Med* 2013;19: 1632–1637.
4. Wohlsen A, Martin C, Vollmer E, Branscheid D, Magnussen H, Becker WM, Lepp U, Uhlig S. The early allergic response in small airways of human precision-cut lung slices. *Eur Respir J* 2003;21:1024–1032.
5. Perez JF, Sanderson MJ. The frequency of calcium oscillations induced by 5-HT, ACH, and KCl determine the contraction of smooth muscle cells of intrapulmonary bronchioles. *J Gen Physiol* 2005;125:535–553.
6. Henjakovic M, Sewald K, Switalla S, Kaiser D, Müller M, Veres TZ, Martin C, Uhlig S, Krug N, Braun A. *Ex vivo* testing of immune responses in precision-cut lung slices. *Toxicol Appl Pharmacol* 2008;231:68–76.
7. Fahy GM, Guan N, de Graaf IA, Tan Y, Griffin L, Groothuis GM. Cryopreservation of precision-cut tissue slices. *Xenobiotica* 2013;43: 113–132.
8. Kasper HU, Konze E, Kutinová Canová N, Dienes HP, Dries V. Cryopreservation of precision cut tissue slices (PCTS): investigation of morphology and reactivity. *Exp Toxicol Pathol* 2011;63:575–580.
9. Rosner SR, Ram-Mohan S, Paez-Cortez JR, Lavoie TL, Dowell ML, Yuan L, Ai X, Fine A, Aird WC, Solway J, *et al*. Airway contractility in the precision-cut lung slice after cryopreservation. *Am J Respir Cell Mol Biol* 2014;50:876–881.
10. Pegg DE. Principles of cryopreservation. *Methods Mol Biol* 2015;1257:3–19.
11. Gao D, Critser JK. Mechanisms of cryoinjury in living cells. *ILAR J* 2000; 41:187–196.
12. Meryman HT. Cryopreservation of living cells: principles and practice. *Transfusion* 2007;47:935–945.
13. Liggett SB. Bitter taste receptors in the wrong place: novel airway smooth muscle targets for treating asthma. *Trans Am Clin Climatol Assoc* 2014;125:64–74, discussion 74–75.
14. An SS, Wang WC, Koziol-White CJ, Ahn K, Lee DY, Kurten RC, Panettieri RA Jr, Liggett SB. TAS2R activation promotes airway smooth muscle relaxation despite β(2)-adrenergic receptor tachyphylaxis. *Am J Physiol Lung Cell Mol Physiol* 2012;303:L304–L311.
15. Bergner A, Sanderson MJ. Acetylcholine-induced calcium signaling and contraction of airway smooth muscle cells in lung slices. *J Gen Physiol* 2002;119:187–198.
16. Aggarwal NR, King LS, D'Alessio FR. Diverse macrophage populations mediate acute lung inflammation and resolution. *Am J Physiol Lung Cell Mol Physiol* 2014;306:L709–L725.
17. Lavin Y, Winter D, Blecher-Gonen R, David E, Keren-Shaul H, Merad M, Jung S, Amit I. Tissue-resident macrophage enhancer landscapes are shaped by the local microenvironment. *Cell* 2014;159: 1312–1326.
18. Sathaliyawala T, Kubota M, Yudanin N, Turner D, Camp P, Thome JJ, Bickham KL, Lerner H, Goldstein M, Sykes M, *et al*. Distribution and compartmentalization of human circulating and tissue-resident memory T cell subsets. *Immunity* 2013;38:187–197.
19. Coquet JM, Schuijs MJ, Smyth MJ, Deswarte K, Beyaert R, Braun H, Boon L, Karlsson Hedestam GB, Nutt SL, Hammad H, *et al*. Interleukin-21–producing CD4(+) T cells promote type 2 immunity to house dust mites. *Immunity* 2015;43:318–330.
20. Kudo M, Melton AC, Chen C, Engler MB, Huang KE, Ren X, Wang Y, Bernstein X, Li JT, Atabai K, *et al*. IL-17A produced by αβ T cells drives airway hyper-responsiveness in mice and enhances mouse and human airway smooth muscle contraction. *Nat Med* 2012;18: 547–554.
21. Yu YA, Hotten DF, Malakhau Y, Volker E, Ghio AJ, Noble PW, Kraft M, Hollingsworth JW, Gunn MD, Tighe RM. Flow cytometric analysis of myeloid cells in human blood, bronchoalveolar lavage, and lung tissues. *Am J Respir Cell Mol Biol* 2015.
22. Cooper PR, Panettieri RA Jr. Steroids completely reverse albuterol-induced beta(2)-adrenergic receptor tolerance in human small airways. *J Allergy Clin Immunol* 2008;122:734–740.
23. Deshpande DA, Walseth TF, Panettieri RA, Kannan MS. CD38/cyclic ADP-ribose–mediated Ca^{2+} signaling contributes to airway smooth muscle hyper-responsiveness. *FASEB J* 2003;17:452–454.
24. Ressmeyer AR, Bai Y, Delmotte P, Uy KF, Thistlethwaite P, Fraire A, Sato O, Ikebe M, Sanderson MJ. Human airway contraction and formoterol-induced relaxation is determined by Ca^{2+} oscillations and Ca^{2+} sensitivity. *Am J Respir Cell Mol Biol* 2010;43:179–191.
25. Prakash YS, Pabelick CM, Kannan MS, Sieck GC. Spatial and temporal aspects of ACh-induced $[Ca^{2+}]_i$ oscillations in porcine tracheal smooth muscle. *Cell Calcium* 2000;27:153–162.
26. Berridge MJ. Smooth muscle cell calcium activation mechanisms. *J Physiol* 2008;586:5047–5061.
27. Baatz JE, Newton DA, Riemer EC, Denlinger CE, Jones EE, Drake RR, Spyropoulos DD. Cryopreservation of viable human lung tissue for versatile post-thaw analyses and culture. *In Vivo* 2014;28:411–423.
28. Bakhach J. The cryopreservation of composite tissues: principles and recent advancement on cryopreservation of different type of tissues. *Organogenesis* 2009;5:119–126.
29. MacRae JW, Tholpady SS, Ogle RC, Morgan RF. *Ex vivo* fat graft preservation: effects and implications of cryopreservation. *Ann Plast Surg* 2004;52:281–282, discussion 283.
30. Maas WJ, Leeman WR, Groten JP, van de Sandt JJ. Cryopreservation of precision-cut rat liver slices using a computer-controlled freezer. *Toxicol In Vitro* 2000;14:523–530.

31. Mukherjee S, Trice J, Shinde P, Willis RE, Pressley TA, Perez-Zoghbi JF. Ca^{2+} oscillations, Ca^{2+} sensitization, and contraction activated by protein kinase C in small airway smooth muscle. *J Gen Physiol* 2013;141:165–178.
32. Perez-Zoghbi JF, Sanderson MJ. Endothelin-induced contraction of bronchiole and pulmonary arteriole smooth muscle cells is regulated by intracellular Ca^{2+} oscillations and Ca^{2+} sensitization. *Am J Physiol Lung Cell Mol Physiol* 2007;293:L1000–L1011.
33. Chiba Y, Nakazawa S, Todoroki M, Shinozaki K, Sakai H, Misawa M. Interleukin-13 augments bronchial smooth muscle contractility with an up-regulation of RhoA protein. *Am J Respir Cell Mol Biol* 2009;40:159–167.
34. Lan B, Deng L, Donovan GM, Chin LY, Syyong HT, Wang L, Zhang J, Pascoe CD, Norris BA, Liu JC, *et al*. Force maintenance and myosin filament assembly regulated by Rho-kinase in airway smooth muscle. *Am J Physiol Lung Cell Mol Physiol* 2015;308:L1–L10.
35. Artamonov MV, Momotani K, Stevenson A, Trentham DR, Derewenda U, Derewenda ZS, Read PW, Gutkind JS, Somlyo AV. Agonist-induced Ca^{2+} sensitization in smooth muscle: redundancy of Rho guanine nucleotide exchange factors (RhoGEFs) and response kinetics, a caged compound study. *J Biol Chem* 2013;288:34030–34040.
36. Bai Y, Sanderson MJ. Modulation of the Ca^{2+} sensitivity of airway smooth muscle cells in murine lung slices. *Am J Physiol Lung Cell Mol Physiol* 2006b;291:L208–L221.
37. Somlyo AP, Somlyo AV. Ca^{2+} sensitivity of smooth muscle and nonmuscle myosin II: modulated by G proteins, kinases, and myosin phosphatase. *Physiol Rev* 2003;83:1325–1358.
38. Gosens R, Stelmack GL, Dueck G, Mutawe MM, Hinton M, McNeill KD, Paulson A, Dakshinamurti S, Gerthoffer WT, Thliveris JA, *et al*. Caveolae facilitate muscarinic receptor-mediated intracellular Ca^{2+} mobilization and contraction in airway smooth muscle. *Am J Physiol Lung Cell Mol Physiol* 2007;293:L1406–L1418.
39. Delmotte P, Sanderson MJ. Effects of formoterol on contraction and Ca^{2+} signaling of mouse airway smooth muscle cells. *Am J Respir Cell Mol Biol* 2010;42:373–381.
40. Bai Y, Sanderson MJ. Airway smooth muscle relaxation results from a reduction in the frequency of Ca^{2+} oscillations induced by a cAMP-mediated inhibition of the IP3 receptor. *Respir Res* 2006;7:34.
41. Morgan SJ, Deshpande DA, Tiegs BC, Misior AM, Yan H, Hershfeld AV, Rich TC, Panettieri RA, An SS, Penn RB. β-agonist–mediated relaxation of airway smooth muscle is protein kinase A–dependent. *J Biol Chem* 2014;289:23065–23074.
42. McGraw DW, Elwing JM, Fogel KM, Wang WC, Glinka CB, Mihlbachler KA, Rothenberg ME, Liggett SB. Crosstalk between Gi and Gq/Gs pathways in airway smooth muscle regulates bronchial contractility and relaxation. *J Clin Invest* 2007;117: 1391–1398.
43. Delmotte P, Ressmeyer AR, Bai Y, Sanderson MJ. Mechanisms of airway smooth muscle relaxation induced by beta2-adrenergic agonists. *Front Biosci (Landmark Ed)* 2010;15:750–764.
44. Robinett KS, Koziol-White CJ, Akoluk A, An SS, Panettieri RA Jr, Liggett SB. Bitter taste receptor function in asthmatic and nonasthmatic human airway smooth muscle cells. *Am J Respir Cell Mol Biol* 2014;50:678–683.
45. Deshpande DA, Wang WC, McIlmoyle EL, Robinett KS, Schillinger RM, An SS, Sham JS, Liggett SB. Bitter taste receptors on airway smooth muscle bronchodilate by localized calcium signaling and reverse obstruction. *Nat Med* 2010;16:1299–1304.
46. Tan X, Sanderson MJ. Bitter tasting compounds dilate airways by inhibiting airway smooth muscle calcium oscillations and calcium sensitivity. *Br J Pharmacol* 2014;171:646–662.